ChemComm

Dynamic Article Links

Cite this: *Chem. Commun.*, 2011, **47**, 9438–9440

www.rsc.org/chemcomm

COMMUNICATION

Superior energy capacity of graphene nanosheets for a nonaqueous lithium-oxygen battery†

Yongliang Li, Jiajun Wang, Xifei Li, Dongsheng Geng, Ruying Li and Xueling Sun*

Received 12th June 2011, Accepted 9th July 2011
DOI: 10.1039/c1cc13464g

Graphene nanosheets (GNSs) were synthesized and used as cathode active materials in a nonaqueous lithium-oxygen battery. The GNSs electrode delivered an extremely high discharge capacity in comparison to carbon powders, which is attributed to its unique morphology and structure.

The nonaqueous lithium-oxygen/air battery is one of the most promising energy storage systems for hybrid electric vehicles (HEVs) and electric vehicles (EVs) because of its extremely high theoretical energy density.[1] The porosity of the air electrode plays an important role in the lithium-air battery performance because the insoluble products are deposited in the electrode, which block O_2 from diffusing to the reaction sites.[2] Recent work also showed that the oxygen reduction reaction (ORR) in the carbon electrode significantly affected its performance.[3] Therefore, it is important to develop new carbon electrodes to improve the kinetics and enhance the energy capacity.

Graphene nanosheets (GNSs) have attracted great attention for energy storage applications.[4] Especially, they have been widely used as catalyst supports or non-noble catalysts for fuel cells.[5] Recently, Yoo and Zhou examined the GNSs as air electrodes in lithium-air batteries with a hybrid electrolyte and found that GNSs showed good electrocatalytic activity for ORR in an aqueous electrolyte, resulting in high performance.[6] They also developed an idea of applying a graphene-like thin film on a ceramic state electrolyte in a lithium-air battery.[7] However, to the best of our knowledge, no research on GNSs as a cathode for nonaqueous lithium-oxygen batteries has been reported.

Herein, for the first time, we employed GNSs as cathode active materials in nonaqueous lithium-oxygen batteries and found that GNSs delivered an extremely high discharge capacity.

Fig. 1 shows the discharge/charge curves of the lithium-oxygen batteries with GNSs, BP-2000 and Vulcan XC-72 as cathodes at a current density of 75 mA g^{-1}. The discharge capacities of the BP-2000 and Vulcan XC-72 electrodes are 1909.1 and 1053.8 mAh g^{-1}, respectively. The GNSs electrode delivers a capacity of 8705.9 mAh g^{-1}, which is the highest capacity of any carbon-based materials in lithium-oxygen batteries ever reported so far. Moreover, it also shows higher average discharge plateau voltage and charge capacity than BP-2000 and Vulcan XC-72 electrodes, indicating a higher catalytic activity for cathode reactions.[3]

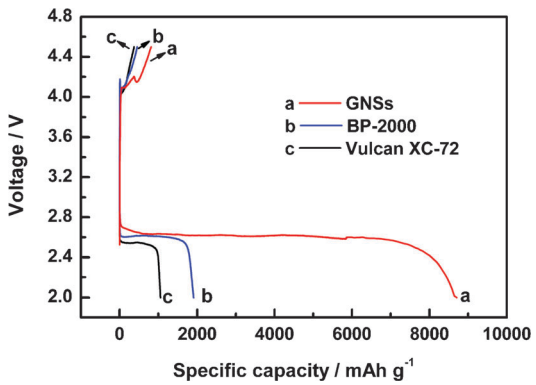

Fig. 1 Discharge–charge performance of lithium-oxygen batteries with (a) GNSs, (b) BP-2000, and (c) Vulcan XC-72 cathodes at a current density of 75 mA g^{-1}.

The SEM and TEM images of GNSs electrode before and after discharge are shown in Fig. 2. As shown in Fig. 2a and b,

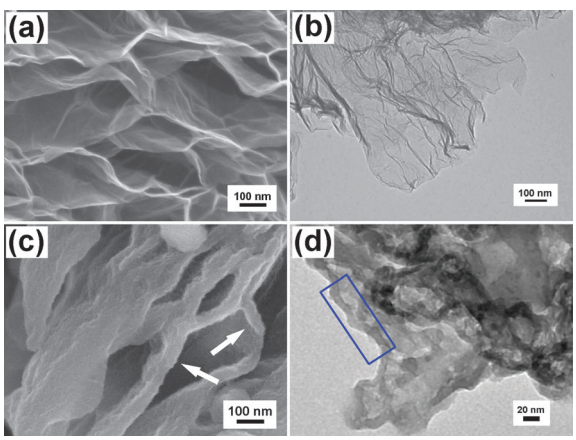

Fig. 2 SEM and TEM images of GNSs electrodes before (a and b) and after (c and d) discharge.

Department of Mechanical and Materials Engineering, The University of Western Ontario, ON, Canada N6A 5B9. E-mail: xsun@eng.uwo.ca; Fax: +1-519-661-3020; Tel: +1-519-661-2111 ext. 87759

† Electronic supplementary information (ESI) available: Experimental details, data of the physical properties. See DOI: 10.1039/c1cc13464g

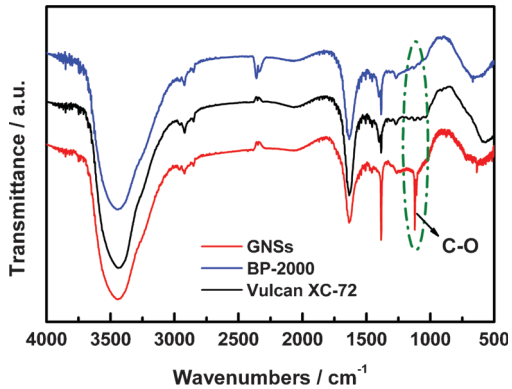

Fig. 3 FTIR spectra of GNSs, BP-2000 and Vulcan XC-72.

the GNSs have a curly morphology with a thin, wrinkled structure.

These unique structures provide ideal porosity which is suitable for the electrolyte wetting and the O_2 diffusion, thus improving the efficiency of the catalyst reactions. The electrode with these structures not only increases the electrochemically accessible site, but also provides a large diffusion path for the O_2 mass transfer, therefore, improving the discharge capacity dramatically.

After discharge, the products deposit on both sides of the GNSs (Fig. 2c), and it is important to note that at the edges of the GNSs, a relatively darker/thicker colour is observed (marked by arrows), suggesting more products on the edge sites as indicated by the square in Fig. 2d.

Fig. 3 shows the FTIR spectra of the GNSs, BP-2000 and Vulcan XC-72. It can be seen that in comparison to the other two carbon materials, GNSs show an extra band at 1120 cm^{-1}, which corresponds to the C–O stretching vibrations.[8] This is because the edge sites of the GNSs contain a large amount of unsaturated carbon atoms which are highly active to react with oxygen and form oxygen-containing groups. Therefore, the presence of these unsaturated carbon atoms results in high activity for ORR.[9]

Several works have reported that the surface area, pore size and mesopore volume of carbon materials significantly affected the specific capacity of lithium-air batteries.[2] These effects are also investigated in this work.

Fig. 4a shows the N_2 absorption–desorption isotherms at 77 K for GNSs, BP-2000 and Vulcan XC-72. All samples are found to yield a type-I isotherm at low P/P_0, indicating the presence of micropores.[10] For GNSs, the hysteresis loop, in the P/P_0 range of $\sim$0.4–1.0, is indicative of mesoporosity in addition to the presence of microporosity.[11] The hysteresis loop for mesopores shifts to a higher P/P_0 range ($\sim$0.8–1.0) for BP-2000 and Vulcan XC-72, which is associated with the presence of a narrower range of mesopores, with larger diameters.

The pore size distribution (PSD) obtained using the Barrett–Joyner–Halenda (BJH) method for the three carbon materials are shown in Fig. 4b. In the mesopore size range (2–50 nm), the GNSs show a wide distribution of pore sizes and much higher pore volume at the pore size range from 2–20 nm, while at large pore size range (20–50 nm), BP-2000 possesses large pore volume. Vulcan XC-72 possesses small pore volume, compared to GNS and BP-2000.

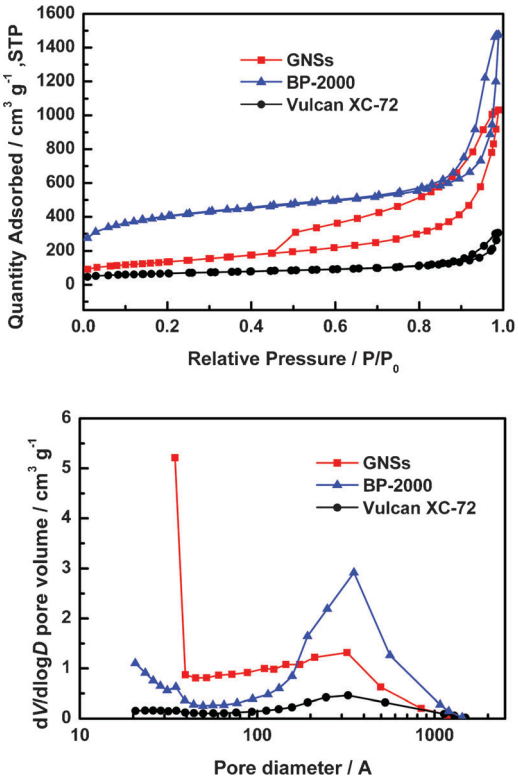

Fig. 4 (a) N_2 adsorption–desorption isotherms at 77 K and (b) pore size distribution (PSD) for GNSs, BP-2000 and Vulcan XC-72.

GNSs have similar mesopore volume but smaller surface area compared to BP-2000 (Table S1, ESI†), while the discharge capacity is much higher. Therefore, the pore size of GNSs plays a more important role in its superior performance, in addition to its novel structure. GNSs possess wide PSD in the mesopore range, forming suitable diffusion channels for the electrolyte and O_2, which is an ideal 3-dimentional (3D), 3-phase electrochemical area.[12]

Fig. 5 shows the XRD pattern of the GNSs electrode after discharge. The dominant discharge product is Li_2CO_3 and a small amount of Li_2O_2 is also present. Xiao and Zhang *et al.* and Bruce *et al.* have reported that for a carbon-based electrode, the formation of Li_2CO_3, along with a small amount of Li_2O_2, was because the intermediate product of

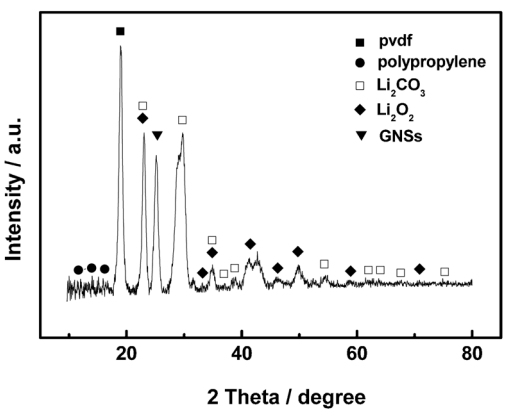

Fig. 5 XRD pattern of GNSs electrode after discharge.

the reaction between Li and O_2 may in turn react with the carbonate solvent in the PC/EC-based electrolyte.[13]

In summary, GNSs were employed as the cathode materials for lithium-oxygen batteries, and for the first time, were demonstrated to show an excellent electrochemical performance with a discharge capacity of 8705.9 mAh g^{-1}. The unique structures of GNSs form an ideal 3D 3-phase electrochemical area and the diffusion channels for the electrolyte and O_2, which increase the efficiency of the catalyst reaction. In addition, the active sites at the edge significantly contribute to the superior electrocatalytic activity towards ORR. Although the detailed mechanism for the oxygen reduction reaction on GNSs in a nonaqueous electrolyte is unclear, it has revealed that GNSs can deliver an extremely high discharge capacity, showing promising applications in lithium-oxygen batteries.

This research was supported by Natural Sciences and Engineering Research Council of Canada, Canada Research Chair Program, Canada Foundation for Innovation, Ontario Early Researcher Award and the University of Western Ontario.

Notes and references

1 K. Abraham and Z. Jiang, *J. Electrochem. Soc*., 1996, **143**, 1; M. Armand and J.-M. Tarascon, *Nature*, 2008, **451**, 652; T. Zhang, N. Imanishi, Y. Shimonishi, A. Hirano, Y. Takeda, O. Yamamoto and N. Sammes, *Chem. Commun*., 2010, **46**, 1661; K. Takechi, T. Shiga and T. Asaoka, *Chem. Commun*., 2011, **47**, 3463.

2 J. Xiao, D. Wang, W. Xu, D. Wang, R. Williford, J. Liu and J.-G. Zhang, *J. Electrochem. Soc*., 2010, **157**, A487; R. Williford and J.-G. Zhang, *J. Power Sources*, 2009, **194**, 1164; X. Yang, P. He and Y. Xia, *Electrochem. Commun*., 2009, **11**, 1127; S. Zhang, D. Foster and J. Read, *J. Power Sources*, 2010, **195**, 1235; M. Mirzaeian and P. Hall, *Electrochim. Acta*, 2009, **54**, 7444.

3 R. Padbury and X. Zhang, *J. Power Sources*, 2011, **196**, 4436; Y.-C. Lu, H. Gasteiger and Y. Shao-Horn, *Electrochem. Solid-State Lett*., 2011, **14**, A70; A. Débart, A. Paterson, J. Bao and P. Bruce, *Angew. Chem., Int. Ed*., 2008, **47**, 4521; H. Cheng and K. Scott, *J. Power Sources*, 2010, **195**, 1370; P. Kichambare, J. Kumar, S. Rodrigues and B. Kumar, *J. Power Sources*, 2011, **196**, 3310; Y. Li, J. Wang, X. Li, D. Geng, J. Yang, R. Li and X. Sun, *Electrochem. Commun*., 2011, **13**, 668.

4 J. Choi, J. Jin, I. Jung, J. Kim, H. Kim and S. Son, *Chem. Commun*., 2011, **47**, 5241; H. Wang, C. Zhang, Z. Liu, L. Wang, P. Han, H. Xu, K. Zhang, S. Dong, J. Yao and G. Cui, *J. Mater. Chem*., 2011, **21**, 5430; K. Chang and W. Chen, *Chem. Commun*., 2011, **47**, 4252; Q. Yue, K. Zhang, X. Chen, L. Wang, J. Zhao, J. Liu and J. Jia, *Chem. Commun*., 2010, **46**, 3369.

5 Y. Zhou, J. Chen, F. Wang, Z. Sheng and X. Xia, *Chem. Commun*., 2010, **46**, 5951; Y. Shao, S. Zhang, M. Engelhard, G. Li, G. Shao, Y. Wang, J. Liu, I. Aksay and Y. Lin, *J. Mater. Chem*., 2010, **20**, 7491; D. Geng, Y. Chen, Y. Chen, Y. Li, R. Li, X. Sun, S. Ye and S. Knights, *Energy Environ. Sci*., 2011, **4**, 760; L. Qu, Y. Liu, J. Baek and L. Dai, *ACS Nano*, 2010, **4**, 1321.

6 E. Yoo and H. Zhou, *ACS Nano*, 2011, **5**, 3020.

7 Y. Wang and H. Zhou, *Energy Environ. Sci*., 2011, **4**, 1704.

8 S. Stankovich, R. Piner, S. Nguyen and R. Ruoff, *Carbon*, 2006, **44**, 3342.

9 E. Yeager, *J. Mol. Catal*., 1986, **38**, 5; C. Banks, T. Davies, G. Wildgoose and R. Compton, *Chem. Commun*., 2005, (7), 829.

10 M. Kruk, M. Jaroniec and K. Gadkaree, *J. Colloid Interface Sci*., 1997, **192**, 250.

11 Y. Fang, D. Gu, Y. Zou, Z. Wu, F. Li, R. Che, Y. Deng, B. Tu and D. Zhao, *Angew. Chem., Int. Ed*., 2010, **49**, 7987.

12 C. Tran, X. Yang and D. Qu, *J. Power Sources*, 2010, **195**, 2057.

13 J. Xiao, J. Hua, D. Wang, D. Hu, W. Xu, G. Graff, Z. Nie, J. Liu and J.-G. Zhang, *J. Power Sources*, 2011, **196**, 5674; S. Freunberger, Y. Chen, Z. Peng, J. Griffin, L. Hardwick, F. Bardé, P. Novák and P. Bruce, *J. Am. Chem. Soc*., 2011, **133**, 8040.

